

CWDM self-referencing sensor network based on ring resonators in reflective configuration

J. Montalvo, C. Vázquez, D. S. Montero



Displays and Photonics Applications Group, Electronics Technology Department, Carlos III University of Madrid, C/. Butarque 15, 28911 Leganés, Spain

julio.montalvo@uc3m.es, cvazquez@ing.uc3m.es, dsmontero@ing.uc3m.es

Abstract: A new scalable self-referencing sensor network with low insertion losses implemented in Coarse Wavelength Division Multiplexing (CWDM) technology is reported. It allows obtaining remote self-referenced measurements with a full-duplex fibre download up to 35 km long, with no need for optical amplification. Fibre Bragg gratings (FBG) are used in order to achieve a reflective configuration, thus increasing the sensitivity of the optical transducers. Low-cost off-the-shelf devices in CWDM technology can be used to implement and scale the network. Ring resonator (RR) based incoherent interferometers at the measuring points are used as selfreferencing technique. A theoretical analysis of power budget of the topology is reported, with a comparison between the proposed network and a conventional star topology. Finally, the new configuration has been experimentally demonstrated.

OCIS codes: (060.2370) Fiber optics sensors; (060.4230) Multiplexing; (060.4250) Networks; (230.1480) Bragg reflectors; (280.0280) Remote sensing.

References and Links

1. J.M. Baptista, J.L. Santos, A.S. Lage, "Mach-Zehnder and Michelson topologies for self-referencing fiber optic intensity sensors," *Opt. Eng.* **39**, 1636-1644 (2000).
2. C. Vázquez, J. Montalvo, P.C. Lallana, "Radio-Frequency Ring Resonators for Self-Referencing Fibre-Optic Intensity Sensors," *Opt. Eng. Lett.* **44**, 1-2, (2005).
3. R.I. MacDonald, R. Nychka, "Differential Measurement Technique for Optical Fibre Sensors," *Electron. Lett.* **27**, 2194-2196 (1991).
4. S. Diaz, M. López-Amo, "Comparison of WDM distributed fiber Raman amplifier networks for sensors," *Opt. Express* **14**, 1401-1407 (2006).
5. S. Abad, M. López-Amo, "Single and double distributed optical amplifier fiber bus networks with wavelength-division multiplexing for photonic sensors," *Optics Letters* **24**, 805-807 (1999).
6. S. Abad, M. López-Amo, "Fiber Bragg grating-based self-referencing technique for wavelengthmultiplexed intensity sensors," *Opt. Lett.* **27**, 222-224 (2002).
7. J.Montalvo, C.Vázquez, D.S. Montero, "Frequency response of two ring-resonators in series using fibre Bragg Gratings," in *Proc. Fourth Spanish Meeting on Optoelectronics (OPTOEL 05)*, pp. 201-205 (2005).
8. C.Vázquez, J.Montalvo, D.S. Montero, Electronics Technology Department, Carlos III University of Madrid, 15 Butarque Street, Leganés, Madrid, are preparing a manuscript to be called "Self-referencing fiber-optic intensity sensors using Ring Resonators and Fibre Bragg Gratings".

1. Introduction

Fibre-optic sensors (FOS) can operate at hostile and flammable environments and also in the presence of electromagnetic interference. In the case of optical intensity-based transducers, changes of optical power are related directly to the external magnitude to measure. But these variations could have a different origin than the magnitude of interest, because of unpredictable changes in losses of passive components such as fibre leads, optical couplers or connectors, which may change in time and because of aging and environmental conditions.

Additionally, random power fluctuations of optical sources at the input of the network and detector sensitivity changes can induce an intensity noise added to the desired signals. In order to neutralize all these effects, a variety of self-referencing techniques for intensity sensors have been reported using Michelson and Mach-Zehnder configurations [1] with multimode (MM) fibres, and RR configurations with single mode (SM) [2] and plastic optical fibres [3].

Scalable multiplexing schemes to increase the number of sensors and to reduce the number of components have also been a motive of study between researchers. Reflective configurations, typically using FBG at the measuring points, have been proposed to avoid the need for an additional download fibre. Another object of study has been the power budget enhancement. Bus and star reflective topologies using FBG have been reported [4,5], employing optical amplification in order to compensate insertion losses of optical couplers; nevertheless, the noise associated to amplification is a limiting aspect. Partial optimizations of power budget using WDM devices at the reception stage have been demonstrated in selfreferencing intensity networks [6], but the use of couplers leads to lossy distribution of lightwave channels.

In this paper, a passive intensity sensor multiplexing topology with insertion losses enhancement and self-referenced measurements is demonstrated. The use of CWDM equipment allows optimizing the power budget, thus increasing the number of multiplexed sensors or the distance between the light sources and the remote measuring points. Hybrid CWDM-DWDM stars employing either Arrayed Waveguide Gratings (AWG) or conventional power couplers at the last stages of the proposed topology can be used to increase the number of channels keeping cost budget, see Fig. 4. This allows the use of a large number of DWDM carriers in a single CWDM channel reserved bandwidth, still taking advantage of power distribution improvement, and overcoming the restriction in the number of sensors because of the high spectral separation between CWDM channels. Ring resonator (RR) based interferometers at the measuring points are used, with an intensity-based optical sensor placed in the loop. The use of external FBG attached to the RR allows achieving the reflective topology and increasing the sensitivities of the optical transducers. The proposed topology can also be applied to any frequency based self-referencing optical configuration emplaced at the measuring points, such as Mach-Zehnder and Michelson interferometers.

2. CWDM sensor network configuration

A diagram of the proposed network topology is shown in Fig. 1.

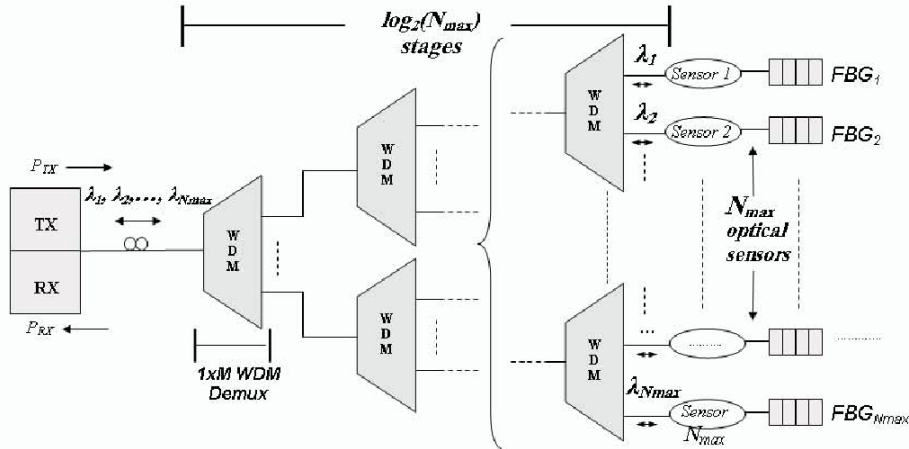


Fig. 1. Proposed passive CWDM star network for intensity sensors.

In the transmission-reception (TX/RX) central unit, the CWDM channels are multiplexed into a full-duplex fibre-optic lead, which links the TX/RX central with the remote measuring points where the different optical intensity sensors are emplaced. One CWDM optical channel is dedicated to each intensity sensor, leading optical power specifically to each sensor by a cascade of WDM demultiplexers, with no other accumulated losses that propagation and non-

ideal behavior of the devices. This provides a power budget enhancement which allows increasing the main link distance with no optical amplification.

The higher the number of output channels of the WDM demultiplexers (M), the lower the number of stages required to distribute the lightwave to the N_{max} sensors. The optimal situation is a single WDM stage with a low-cost CWDM mux/demux device with N_{max} output ports, distributing specifically each CWDM channel to its optical sensor.

The reflective configuration is achieved by emplacing a FBG at each measuring point, reflecting specifically the CWDM channel dedicated to each sensor. Ring resonator based incoherent interferometers are used to achieve a self-referencing technique [2]. Optical channels return back to the central unit after a second passing through each intensity sensor, thus increasing the transducer intrinsic sensitivity.

The same bidirectional WDM series of devices with the same propagation and low insertion losses provides the return path for the CWDM channels to the TX/RX unit, where the counter-propagating signals in the main fibre lead are discriminated with a WDM circulator and demultiplexed at the reception stage.

3. Theoretical analysis of power budget

In this section we study comparatively the end-to-end insertion losses of the proposed network in the particular case of using 1x2 WDM demultiplexers ($M=2$), which is directly comparable to the conventional topology where 3dB couplers in cascade are used (see Fig. 2), as in the reported network of [4] with Raman amplification.

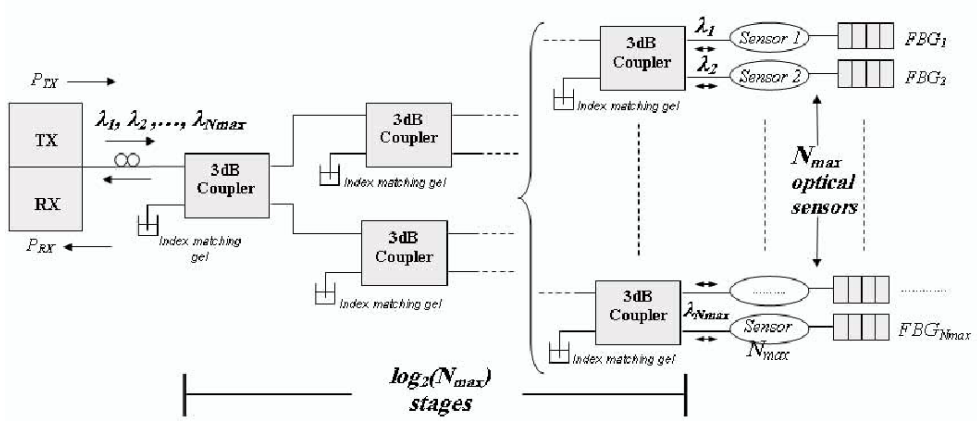


Fig. 2. Passive WDM star topology for intensity sensors using 3 dB couplers.

Assuming a generic scalable star topology with a cascade of CWDM devices to distribute the optical channels to a maximum number of optical sensors N , the final ratio between output optical power () $R_X P$ and input optical power () $T_X P$ is the following:

$$\frac{P_{RX}}{P_{TX}} = \frac{IL_f \cdot \left(10^{-\frac{2\alpha \cdot L_{link}}{10}} \right) \cdot (RR_{IL})^2 \cdot IL_d \cdot R_{FBG}}{\log_2(N)} \quad (1)$$

In Eq. (1), IL_f and IL_d represent the fixed losses at TX/RX central unit and the insertion losses of the devices used to implement the star, respectively; α , L_{link} are the attenuation coefficient of the main fibre lead in dB/km and the lead length in km; RR , $FBG R$ are the intrinsic insertion losses of the self-referencing configuration and the reflection losses of the

FBG.

Two main advantages in comparison with a 3dB couplers in cascade similar network arise from this analysis. Firstly, Eq. (1) shows that losses increase with $2^{\max \log N}$, while in a similar star topology using couplers [4] instead of CWDM, they increase with $2^{\max N}$, leading to a lower power budget for the same number of sensors. In the general case, the number of distribution stages using CWDM devices is $\max \log_M N$, so the required stages to multiplex N_{\max} sensors can be reduced by increasing the number of ports of the demultiplexers (M).

The second advantage of the proposed configuration is that αIL is around 0.6 dB when CWDM demultiplexers are used, while losses in a 3 dB coupler are at least 6 dB (forward and reverse directions). The comparison between both networks for the same detector sensitivity and $M=2$ is shown graphically in Fig. 3.

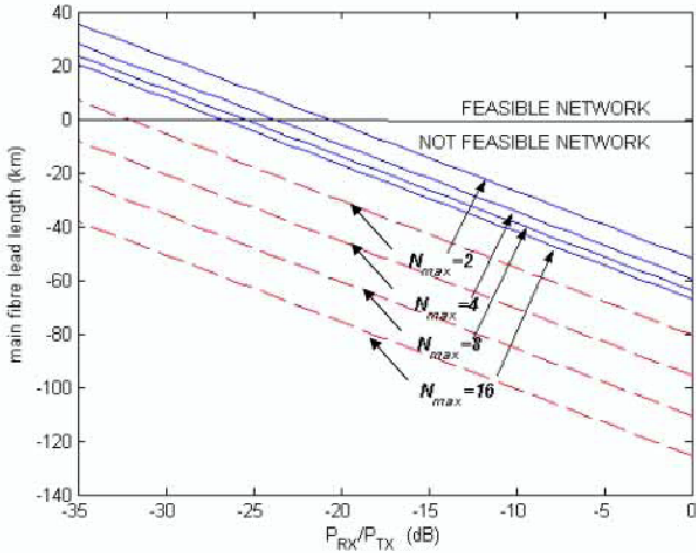


Fig. 3. Maximum fibre lead lengths of star topologies using a 2-CWDM cascade (continuous line) and using 3dB 2x2 couplers (dashed line).

In Fig. 3 the maximum values of the main fibre lead length are represented against the total insertion losses, for the two network schemes under comparison, and for the maximum number of multiplexed optical transducers on the G.694.2 spectral grid. A horizontal line divides the graph into two different regions; the upper one includes possible implementations of the topologies, while the region at the bottom suggests that impossible negative distances would be required for an implementation, which is consequently not feasible. Therefore, the implementation of the proposed network with cascaded 3dB couplers would have been impossible for the imposed restriction without an optical post-amplifier.

It can also be seen that for $N_{\max}=2$ the feasible network in CWDM technology has a maximum download fibre around 30 km longer than the feasible topology involving couplers.

3.1 Scalability in DWDM technology

Although the separation between carriers in the CWDM spectral grid implies a restriction in the maximum number of optical channels employing CWDM technology, the proposed lightwave distribution concept allows using a larger number of Dense WDM carriers within the bandwidth of each CWDM channel at C and L band. By using Arrayed Waveguide Gratings (AWG) or other DWDM devices at the final stage to scale the network (see Fig. 4), low additional insertion losses around 5 dB per propagation sense and per channel would

appear, while several decens of DWDM channels could be used simultaneously.

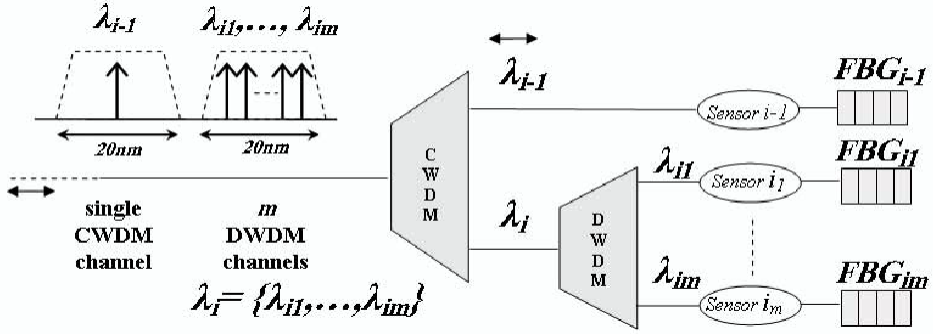


Fig. 4. Last distribution state of DWDM channels for a hybrid CWDM/DWDM topology.

When using DWDM channels, crosstalk caused by limited isolation of DWDM devices and fibre non-linearities such as Stimulated Brillouin Scattering (SBS) should be experimentally explored to preserve the quality of the measurements, specially for a 10 GHz separation between channels, but that is beyond the objects of this paper.

4. The ring resonator configuration with external Bragg gratings

An optical ring resonator with an embedded optical sensor within the recirculating loop is emplaced at each remote measuring point in order to perform a frequency separation technique as self-referencing mechanism.

Reflection at Bragg gratings returns the modulated optical signal back to the ring, obtaining a second-order filter with two identical ring resonators in series equivalent response [7], thus increasing the sensitivity of the optical transducer.

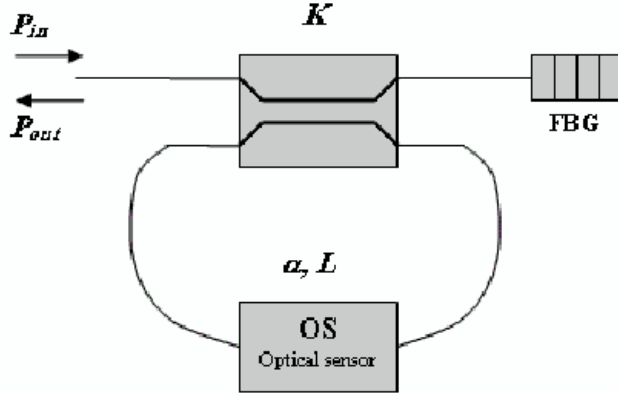


Fig. 5. Remote self-referencing sensor configuration based on RR with fiber Bragg gratings.

In Fig. 5, K is the direct power coupling factor of the optical coupler, L is the loop length and H represents the global recirculating loop power balance:

$$H = 10^{-\alpha L/10} \cdot F(m) \cdot (1 - \gamma) \quad (2)$$

where γ represents the coupler excess losses; α, L are the attenuation coefficient of optical fibre in dB/km and recirculating loop transit time; and finally, $F(m)$ is the optical power

sensor curve as a function of external magnitude, m .

4.1 Ring resonator point of operation

When the optical source coherence length is much lower than loop length L , incoherent optical interference regime is performed in the RR emplaced at the measuring points.

The reflective configuration using FBG optimizes the second-order filter frequency response in terms of symmetry, because the two rings are physically the same, and so the same point of operation for the two equivalent resonators can be achieved with one sole adjusting process as regards coupling factor ($K_1=K_2$) and loop length ($L_1=L_2$). Because of that, the configuration is less sensitive to coupling factor and loop length fabrication tolerances for symmetric bidirectional optical couplers and intensity sensors.

It has been found that a ring resonator close to the notch filter performance provides a good bias point to improve the intrinsic sensitivities of optical transducers [1], so the relationship between K and H must be considered in order to achieve a second-order zero of the power transfer function. This condition is expressed mathematically in Eq. (3) for incoherent regime of interference.

$$H_0 = \frac{K}{1-2 \cdot K} \quad (3)$$

$H_0 = H_{(m=m_0)}$, being m_0 the value of the external magnitude at the bias point.

4.2 Self-referencing measurement parameter with sensitivity improvement

By modulating the optical CWDM channels with two common radio-frequencies (RF) f_1, f_2 and using the ring-resonator-based configuration (see Fig. 4) at the measuring points, a selfreferencing technique to take measurements from optical transducers at each measuring point is achieved. The two radio-frequencies (RF) f_1 and f_2 are used as sensor and reference channels, respectively. The ratio between optical power at those frequencies can provide a self-referenced measurement parameter [1,2]. This ratio proved to be insensitive to crosstalk between adjacent channels, see Fig. 6.

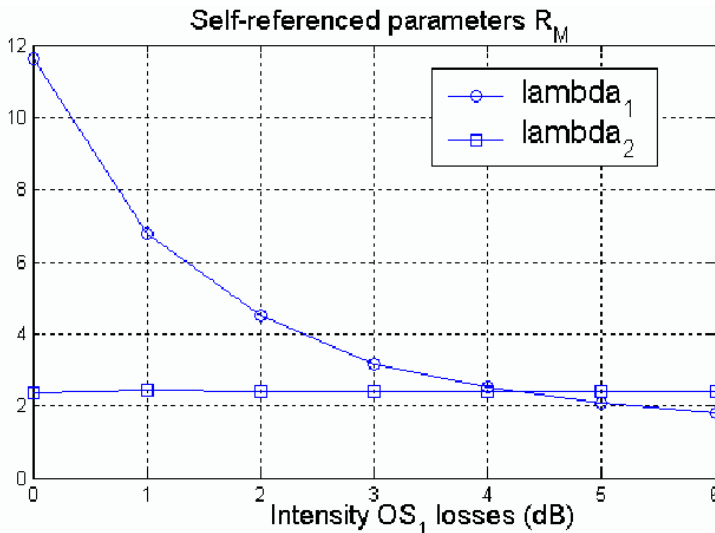


Fig. 6. Evaluation of self-reference parameter crosstalk between two channels at 1530 nm (λ_{1530}) and 1550 nm (λ_{1550}). Separation between RR reference and sensor frequencies: 30% and 40% of RR spectral periodicity, respectively.

To obtain the data of Fig. 6, two different optical sources at 1550 and 1530 nm are externally

modulated simultaneously and injected into a fiber jumper by a 4-CWDM multiplexer. The ratio of the electrical modulation signals between reference and sensor frequencies (R_M) is obtained at every channel after a 4-CWDM demultiplexer, where two output ports are connected to respective fiber-optic ring resonators. This illustrates a case of the topology of Fig. 1, where a single 4-CWDM demultiplexer is employed. Fig. 6 shows how intensity variations for one sensor cause negligible crosstalk in the self-referenced parameter of an adjacent channel, where no intensity variations have been imposed to the respective optical sensor, thus validating the self-referencing technique.

Assuming that input optical power is constant as a function of normalized pulsation $\Omega = 2 \cdot \pi \cdot f \cdot \tau$, being f the modulation RF, the self-referenced parameter to observe for a generic node n is defined as follows:

$$R_{M,n}(\Omega) \equiv \frac{\left| \frac{P_{out,n}}{P_{in,n}} \right|_{z=\exp(j\Omega)}}{\left| \frac{P_{out,n}}{P_{in,n}} \right|_{\substack{z=\exp(j\Omega) \\ \Omega=2 \cdot \pi \cdot f_1 \cdot \tau}}} = \frac{|P_{out,n}(\Omega)|}{|P_{out,n}(\Omega=2 \cdot \pi \cdot f_1 \cdot \tau)|} \quad (8)$$

In Fig. 7, measured and theoretical normalized frequency responses of a RR with and without FBG are represented with good agreement between theory (continuous lines) and measurements (dotted lines). The figure also shows how the ratio between normalized frequency responses of RR and RR+FBG configurations is approximately 2 for any frequency, obtaining a sharper RF response for the latter configuration, as expected

To obtain Fig. 7, a laser diode at 1550 nm was internally modulated by an external tracking generator synchronized with an RF spectrum analyzer, where the represented data were captured via RS-232. More details about the equipment and the components are given in the next section.

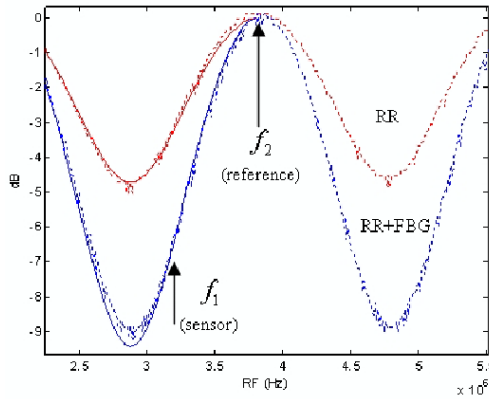


Fig. 7. RR and RR+FBG radio-frequency theoretical (continuous lines) and experimental (dotted lines) normalized responses for a RR and RR+FBG with $K=0.11$, $H=0.6$, $\gamma=0.01$ and 100 meters loop length without optical gain.

5. Experimental set-up and measurement results

In Fig. 8, the scheme of the experimental set up is shown, which is actually a particular implementation of the generic network presented in Fig. 1 with $M=4$ and a single CWDM distribution stage. In order to investigate the feasibility of multiplexing different coarse light sources and implementing simultaneously the RR self-referencing sensor calibration technique using FBG, two distributed-feedback laser diodes at 1530 and 1550 nm emitting 3 dBm were used as RF carriers at the CWDM spectral grid.

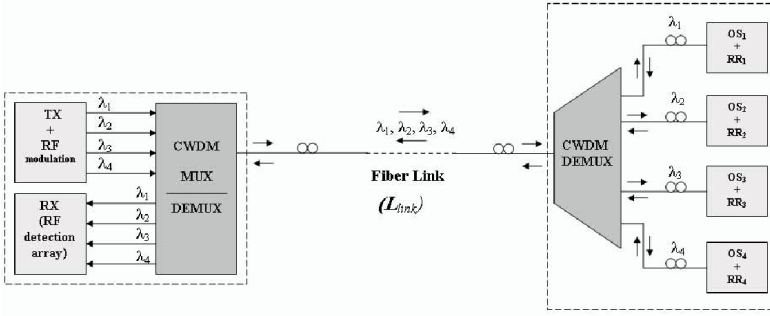


Fig. 8. Scheme of the experimental set up for a 4 CWDM channels sensor network.

The topology shown in Fig. 8 was implemented with standard single-mode fibre with FC/APC connectors, CWDM equipment complying ITU-T G.694.2 recommendation and long-period fibre Bragg gratings. A full-duplex main fibre-optic lead links the TX/RX equipment with the remote measuring points, where the optical intensity sensors embedded in the RR loop are connected to the fibre link by a 4-channels CWDM demultiplexer. The main fibre lead was emulated using a variable attenuator, considering 0.2 dB/km as fibre attenuation coefficient α . The attenuation was adjusted to emulate lengths from 1 km to 35 km ($link L$).

RR loop lengths were 100 meters and optical attenuators were included in the loop to achieve the bias point of the proposed self-referencing technique, simulating generic intensity sensors under a stable environment. No optical amplification was needed and the measurements taken from an Optical Spectrum Analyzer showed a final carrier to noise ratio around 35 dB for a 15 km fibre lead (Fig. 9(a)) with optical crosstalk between adjacent channels below sensitivities of equipment.

In order to obtain the RF responses affecting the two channels and to get the selfreferenced measurement data, the laser diodes were internally modulated by a tracking RF signal synchronized with an spectrum analyzer (Tektronix 2714). An optical to electrical (OE) converter (Thorlabs D400FC) was used to capture the signals in the electrical domain (Fig. 7 and Fig. 9(b)).

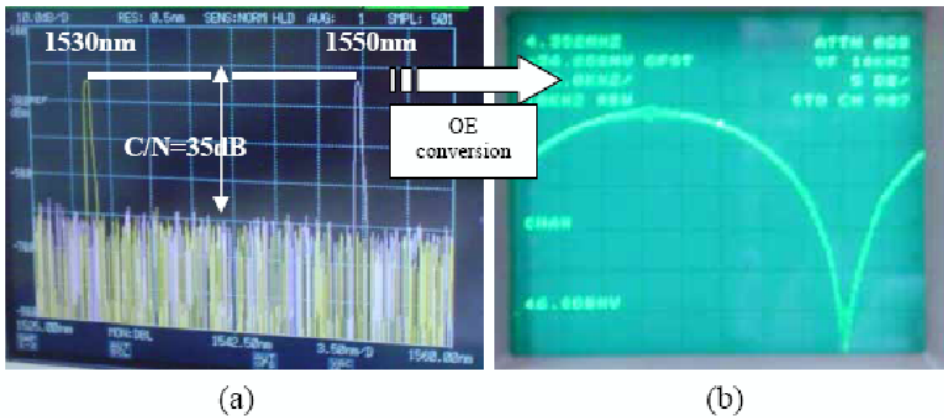


Fig. 9. Optical channels (a) and RF magnitude response @ 1550nm of RR+FBG (b) at reception stage after all network chain of devices and a 15 km main fibre lead. $K=0.26$, $\gamma = 0.01$ and 100m RR fibre loop.

Clean RF magnitude responses corresponding approximately to the RR+FBG configuration were obtained with electrical signal to noise ratios above 20 dB at $f_i = 4.2MHz$ (sensor

frequency) and 30dB at $f = 3.9\text{MHz}$ (reference) for both used CWDM channels. The self-referencing measurement parameter was obtained with relative error noise less than 5%, and revealed to be insensitive to imposed attenuations from 1 to 10 dB of the input power at 1550 nm, simulating power perturbations in the fibre download.

5.1 Power balance and insertion losses optimization

Table 1 shows the different contributions of network elements to the total optical losses, which occurred to be around 25 dB for a 15 km fibre lead. The power budget for the two optical channels at 1530 and 1550 nm was identical except for 0.4 dB. Long period fibre Bragg gratings with reflectivity around 20% (losses of 6 dB) suited the network implementation for a successful global performance.

Table 1. Different losses contributions of the different network devices for the CWDM carrier at 1550nm. The main emulated fibre lead length was approximately 15 km.

CWDM MUX/DEMUX (IL_M)	CWDM DEMUX (IL_{demux})	15 Km main fibre lead	RR + FBG configuration	TX to RX total losses
4.18 dB	0.6 dB	6 dB	14.1 dB	24.88 dB

It can be inferred analytically that the higher the direct coupling factor K is, the lower the RR power insertion losses are in the condition of minima of the magnitude response (see Eq. 3). Optimal RR insertion losses would be reached at $K = 13$ [8], with losses around 5 dB (10 dB for RR+FBG, assuming lossless Bragg reflection). According to this analysis, the RR coupling factor was adjusted to 0.26, near the optimum value of 13, and RR+FBG losses were very close to theoretical calculations.

6. Conclusions

An implementation of a reflective passive star network for intensity sensors employing CWDM equipment to optimize the insertion losses at each optical channel has been reported. It allows an increase of the fibre lead length and the number of multiplexed sensors for passive star networks in reflective configuration of the sensors, obtaining self-referenced measurements with increased sensitivities. Low-cost off-the-shelf devices can be used to implement the topology and to scale the network with more sensors.

A comparative theoretical analysis considering a passive star topology with 3dB couplers has also been presented, concluding that the download length can be 30 km longer by using 2-CWDM demultiplexers instead of couplers.

A real implementation for two multiplexed generic sensors at 1530 and 1550 nm has been demonstrated, with a full-duplex SM fibre link of 15 km and a CWDM demultiplexer as optical distribution stage. The crosstalk between optical channels is around 35 dB, which is a consequence of the isolation ratio of the CWDM demultiplexer. A frequency based selfreferencing technique using RR and FBG has been performed to obtain measurements, which revealed to be insensitive to emulated perturbations of input power from 1 to 10 dB, thus validating the measuring technique. Fibre lead lengths up to 35 km are feasible, but noise at the reception stage provokes an increase of the relative error in the self-referenced measurement parameter, thus making necessary noise reduction techniques.

The proposed topology can be applied to any other frequency-based self-referencing mechanism such as Mach-Zehnder or Michelson configurations. The number of sensors admitted in the new topology can also be scaled easily by replacing one CWDM channel with closer carriers using DWDM technology at the final distribution stages.

Acknowledgments

This work has been supported by CICYT:TIC2003-03783, UC3M:FAVICOBIS and CAM: FACTOTEM-CM (S-0505/ESP/000417). Collaboration in the experimental set up of M.A. González and A. Barragán were most helpful.